Design and Control of the Lift Subsystem of a Two-Wheeled Forklift Robot

Content

Sergio Esteban Quintero Benavides
Keio University
Faculty of Science and Technology
School of Integrated Design Engineering
Murakami Laboratory
2nd year – Master's degree

慶應義塾
Keio University

I. Introduction

In modern industrial environments, humans and robots work together.

- Labor shortage in industrialized countries.
- High-risk tasks executed by robots.

Mobile robots should have a small footprint for safety and space optimization reasons.

[A]

[B]

I. Introduction

Two-Wheeled Forklift Robot:

- Aimed for load movement in warehouses.
- Self-balanced mobile robot.
- Small footprint.

[c]

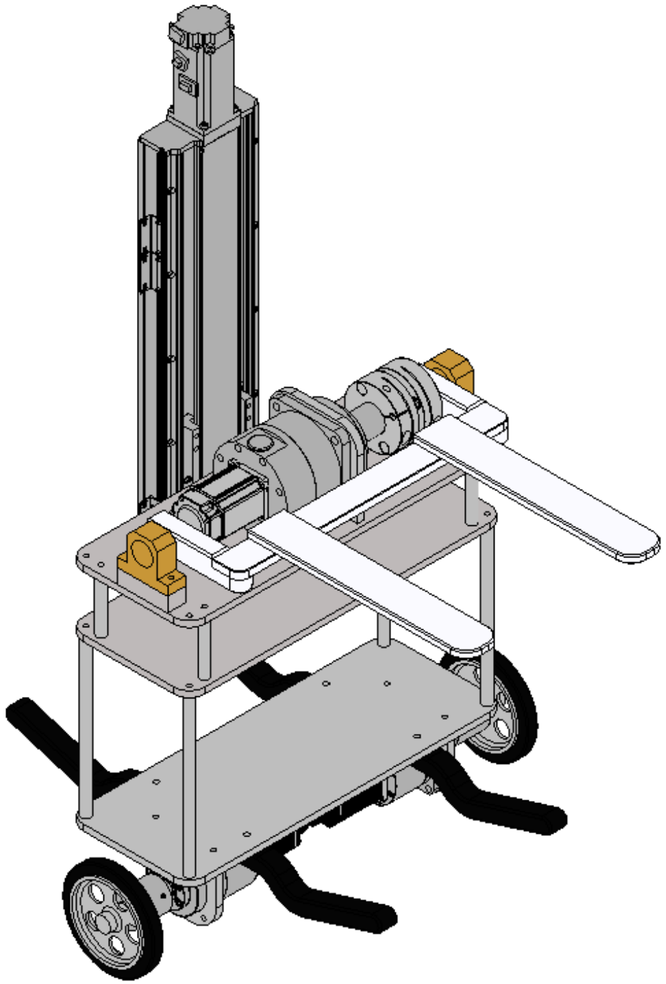

II. Conceptual mechanical design

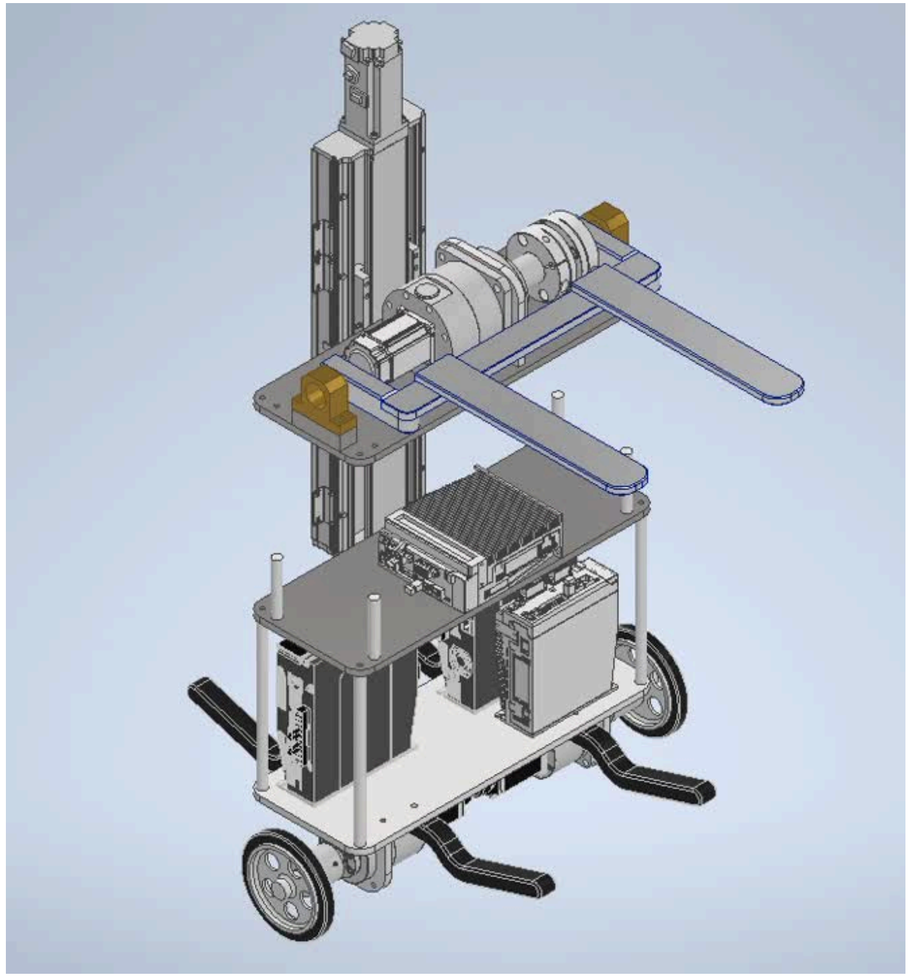

II. Conceptual mechanical design

Ball screw linear actuator ETH2-17-L5-350-BC-M40B-E5N5L

Repeatability		mm	(+/-0.005)			
Lead		mm	5	10	20	40
Maximum Rotating Speed(mm/s)		rpm	3600	3600	3600	3600
Maximum Linear Speed		mm/s	300	600	1200	2400
Maximum Payload	Horizontal	kg	120	110	75	16
	Vertical (For Non-generative power)	kg	40	25	11	9
	Verical(external 50W regenerative registor)	Kg	50	30	18	15
Rated Thurst		N	1389	694	347	174
Stroke Pitch		mm	50-1200mm/50 intervals(50mm pitch)			
Maximum Acceleration		G	0.15	0.31	0.61	1.22
Ball Screw	Basic Dynamic load rating Ca	N	13428	11223	5667	9656
	Basic Static load rating Coa	N	29671	24456	11182	20274
Linear Guide	Dynamic Horizontal	N	7866			
	Static Horizontal	N	78400			
Fixed Bearing	Bsic Dynamic load rating Cr	N	9666			
	Static Load rating Cor	N	6400			
AC Actuator with Motor Output		W	400			
Ball Screw		mm	C7 X ⌀20			
Linear Guide		mm	W15XH12.5			
Ball Screw		mm	14 X 12			
Home Sensor	Outside		T64N2(NPN)			

III. Modeling

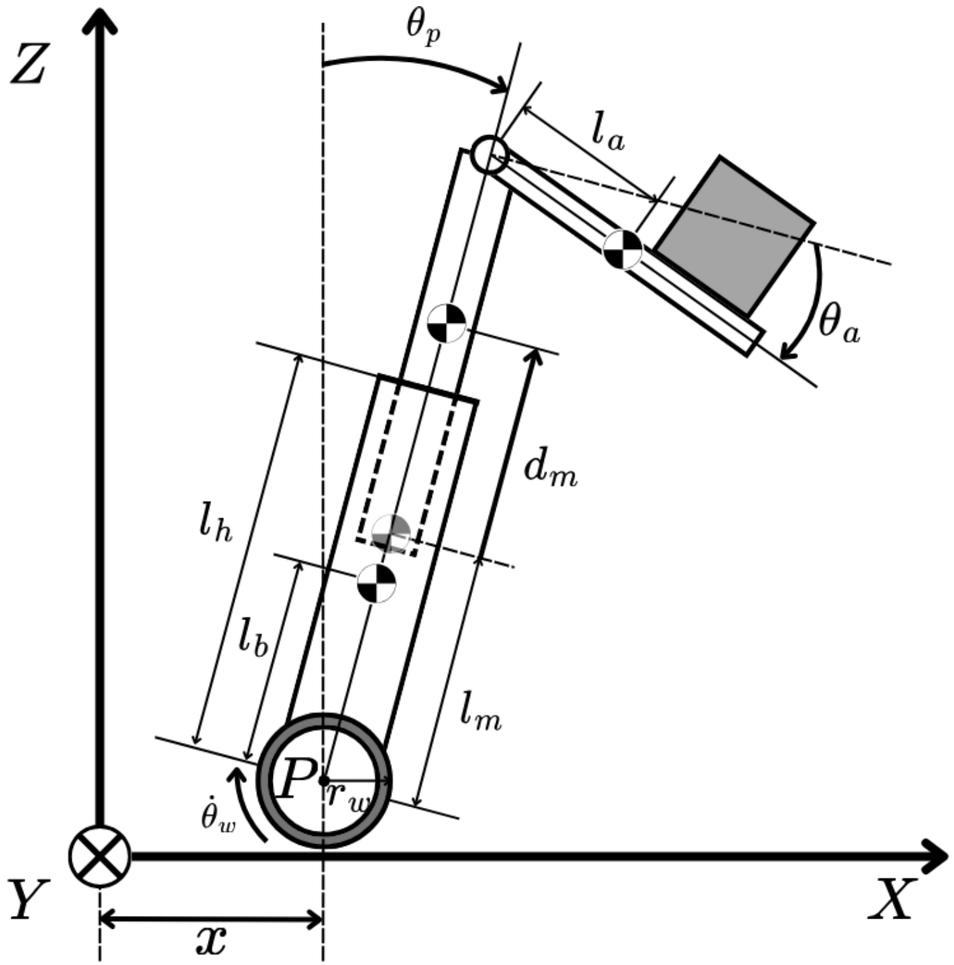

Kinematics:

$$\theta_w : Wheel\ angle, \quad \theta_p : Pitch\ angle,$$
$$d_m : Lift\ displacement, \quad \theta_a : Arm\ angle$$

$$\theta_p + \theta_a = 0$$

$$H_T^B = \begin{pmatrix} 1 & 0 & 0 & s_p(\mathrm{l_h} + d_m) + \mathrm{l_a} \\ 0 & 1 & 0 & 0 \\ 0 & 0 & 1 & r_w + c_p(\mathrm{l_h} + d_m) \\ 0 & 0 & 0 & 1 \end{pmatrix}$$

III. Modeling

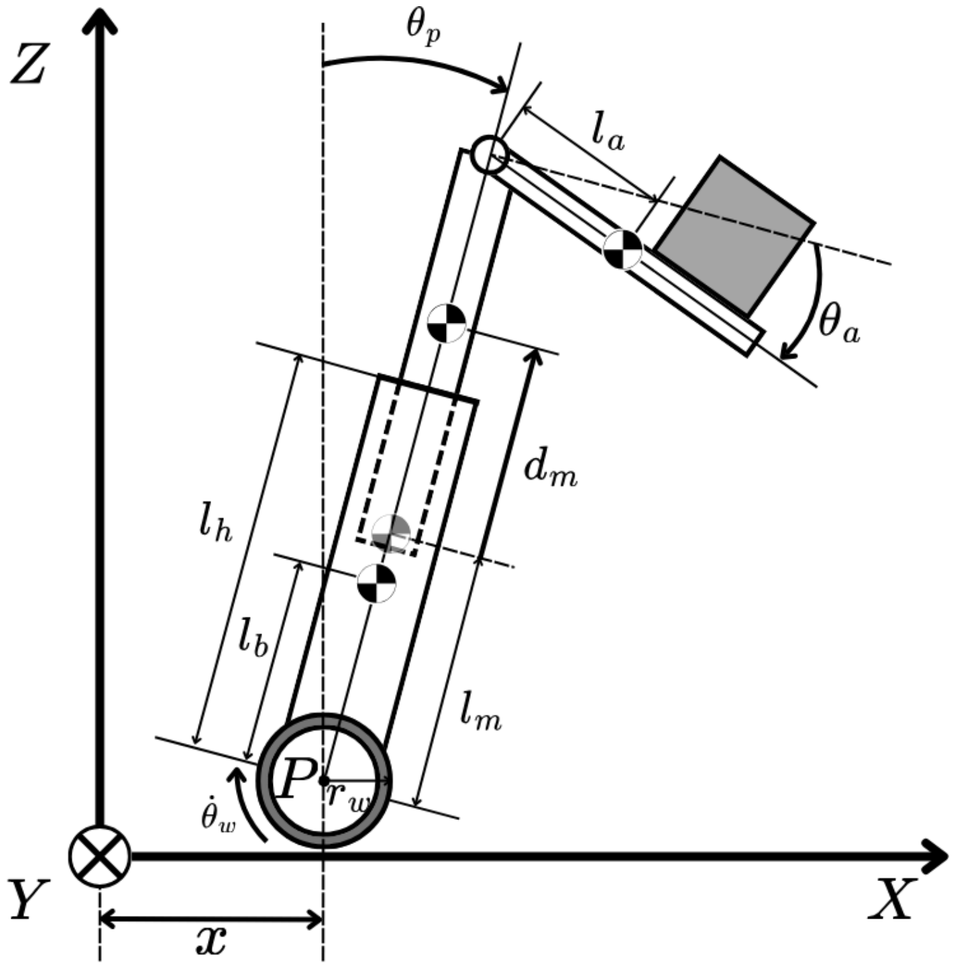

Kinematics:

$$CoG = \begin{pmatrix} \frac{\mathrm{m_l}\left(d_m s_p + \mathrm{l_h} s_p + \frac{\mathrm{t_l}}{g\ \mathrm{m_l}}\right) + \mathrm{m_a}(\mathrm{l_a} + d_m s_p + \mathrm{l_h} s_p) + \mathrm{m_b}\ \mathrm{l_b} s_p + \mathrm{m_m}(d_m + \mathrm{l_m}) s_p}{\mathrm{m_a} + \mathrm{m_b} + \mathrm{m_l} + \mathrm{m_m}} \\ \frac{(\mathrm{m_a} + \mathrm{m_l})\ (d_m c_p + \mathrm{l_h} c_p) + \mathrm{m_b}\ \mathrm{l_b} c_p + \mathrm{m_m}(d_m + \mathrm{l_m}) c_p}{\mathrm{m_a} + \mathrm{m_b} + \mathrm{m_l} + \mathrm{m_m}} \end{pmatrix}$$

$$\begin{cases} r_w + c_p(\mathrm{l_h} + d_m) = z \\ c_p \dot{d}_m - s_p(\mathrm{l_h} + d_m)\dot{\theta}_p = \dot{z} \\ CoG_x(\theta_p, d_m, \mathrm{m_l}, \mathrm{t_l}) = 0 \\ \dot{CoG}_x(\theta_p, \dot{\theta}_p, d_m, \dot{d}_m, \mathrm{m_l}, \mathrm{t_l}) = 0 \end{cases}$$

III. Modeling

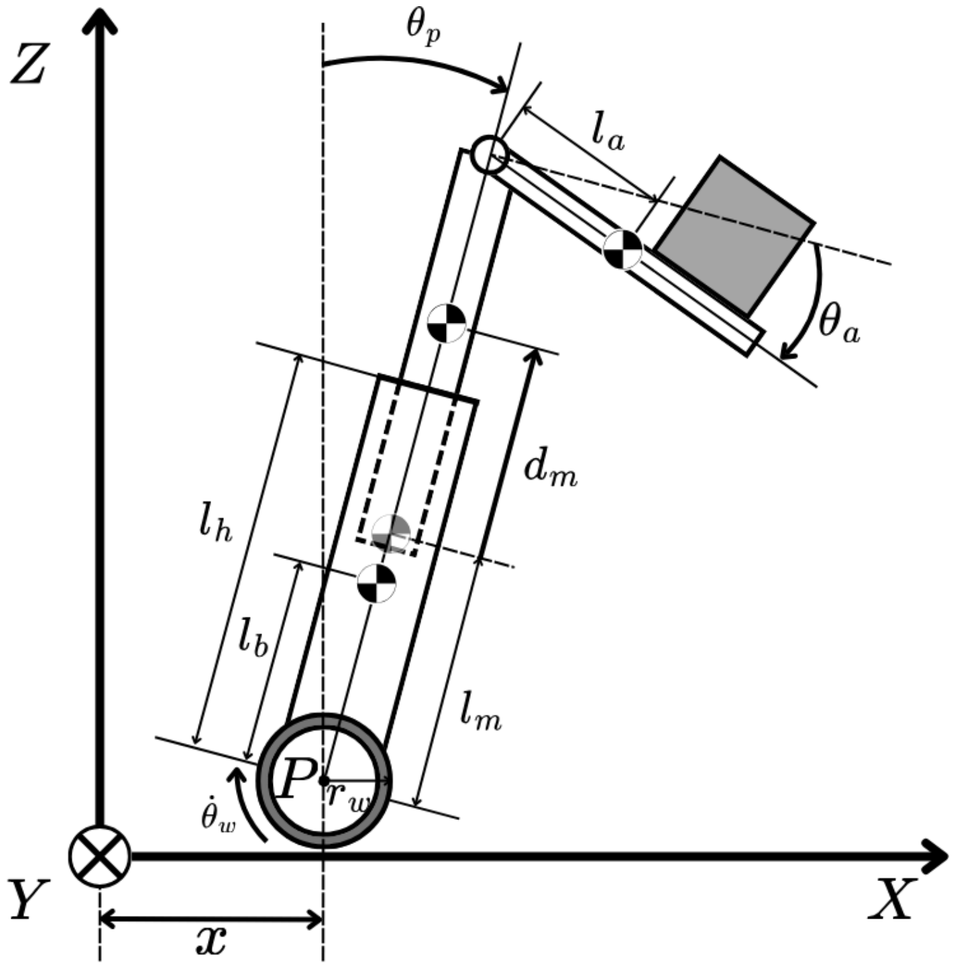

Dynamics:

$$M(q)\ddot{q} + H(\dot{q}, q) + G(q) = \tau$$

Generalized coordinates:

$$q = [\theta_w \quad \theta_p \quad d_m \quad \theta_a]^T$$

$$\tau = [n_w\tau_w \quad -n_w\tau_w \quad f_m \quad n_a\tau_a]^T$$

τ_w : *Wheel torque*, f_m : *Lift force*,

τ_a : *Arm torque*

III. Modeling

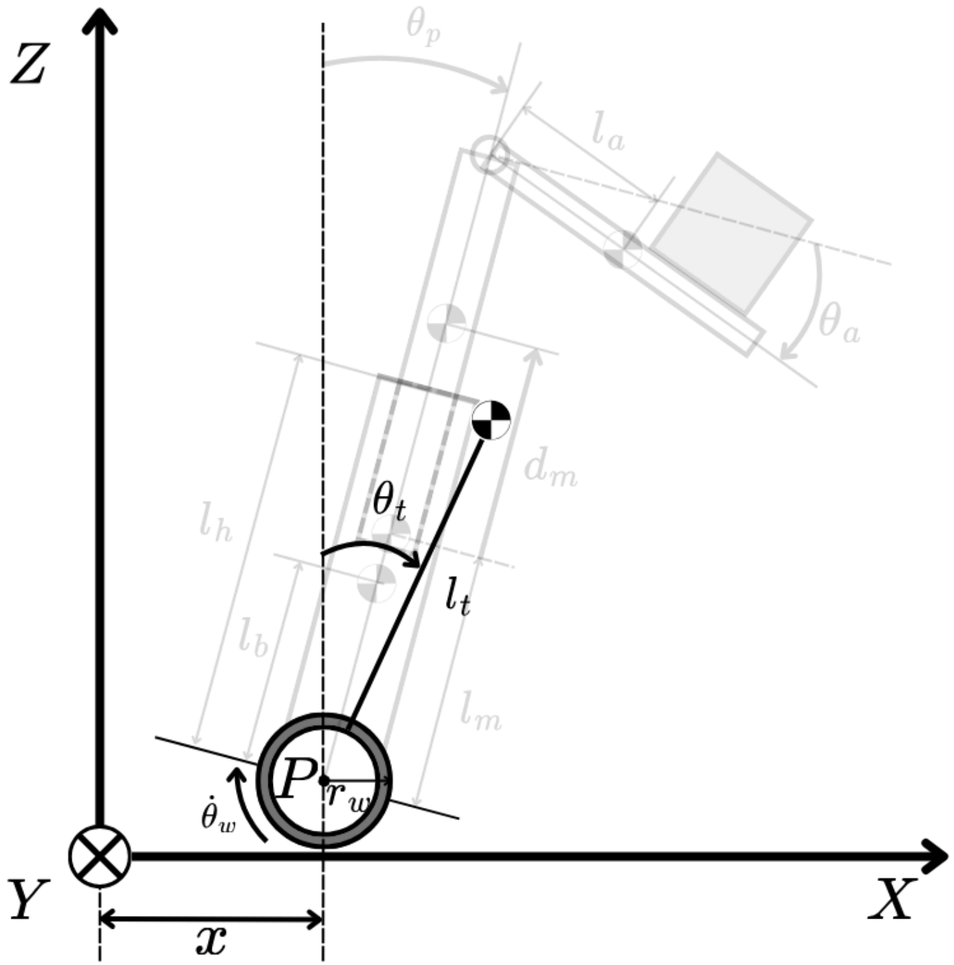

Simplified dynamics:

$$M^*(q')\ddot{q'} + H^*(\dot{q'}, q') + G^*(q') = \tau^*$$

Generalized coordinates:

$$q' = \begin{bmatrix} \theta_w & \theta_t \end{bmatrix}^T$$

$$\tau^* = \begin{bmatrix} n_w \tau_w & -n_w \tau_w \end{bmatrix}^T$$

$$\theta_t = atan(\frac{CoG_x}{CoG_z}), \quad \mathrm{l_t} = \|CoG\|$$

IV. Control

Synthesized Pitch Angle Disturbance Observer (SPADO):

$$m_{11}\ddot{\theta}_w + m_{12}\ddot{\theta}_p + m_{13}\ddot{d}_m + m_{14}\ddot{\theta}_a + h_1 = n_w\tau_w - T_{lw}$$

$$m_{n11}\ddot{\theta}_w^{res} = n_w\tau_w^{ref} - \widetilde{\tau}_w^{dist}$$

$$\widetilde{\tau}_w^{dist} = (m_{11} - m_{n11})\ddot{\theta}_w + m_{12}\ddot{\theta}_p + m_{13}\ddot{d}_m + m_{14}\ddot{\theta}_a + h_1 + T_{lw}$$

$$m_{21}\ddot{\theta}_w + m_{22}\ddot{\theta}_p + m_{23}\ddot{d}_m + m_{24}\ddot{\theta}_a + h_2 + g_2 = -n_w\tau_w - T_{lp}$$

$$m_{n21}\ddot{\theta}_w^{res} + m_{n22}\ddot{\theta}_p^{res} = -n_w\tau_w^{ref} - \widetilde{\tau}_p^{dist}$$

$$\widetilde{\tau}_p^{dist} = (m_{21} - m_{n21})\ddot{\theta}_w + (m_{22} - m_{n22})\ddot{\theta}_p + m_{23}\ddot{d}_m + m_{24}\ddot{\theta}_a + h_2 + g_2 + T_{lp}$$

IV. Control

SPADO:

$$m_{n22}\ddot{\theta}_p^{res} + \frac{m_{n21}+m_{n11}}{m_{n11}} n_w \tau_w^{ref} = \frac{m_{n21}}{m_{n11}}\widetilde{\tau}_w^{dis} - \widetilde{\tau}_p^{dist}$$

$$\widetilde{\tau}_s^{dist} = \widetilde{\tau}_p^{dist} - \frac{m_{n21}}{m_{n11}}\widetilde{\tau}_w^{dis}$$

$$m_{n22}\ddot{\theta}_p^{res} + \frac{m_{n21}+m_{n11}}{m_{n11}} n_w \tau_w^{ref} = -\widetilde{\tau}_s^{dist}$$

$$\hat{\tau}_s^{dist} = \frac{g_s}{s+g_s}\left(g_s m_{n22}\dot{\theta}_p^{res} - \frac{m_{n21}+m_{n11}}{m_{n11}} n_w \tau_w^{ref}\right) - g_s m_{n22}\dot{\theta}_p^{res}$$

Pseudo differentiation

IV. Control

PD controller pitch angle:

$$V = \frac{1}{2}K_1(\theta_p^{cmd} - \theta_p^{res})^2 + \frac{1}{2}K_2(\dot{\theta}_p^{cmd} - \dot{\theta}_p^{res})^2$$

$$\dot{V} = (\dot{\theta}_p^{cmd} - \dot{\theta}_p^{res})(K_1(\theta_p^{cmd} - \theta_p^{res}) + K_2(\ddot{\theta}_p^{cmd} - \ddot{\theta}_p^{res}))$$

$$\dot{V} = -K_3(\dot{\theta}_p^{cmd} - \dot{\theta}_p^{res})^2$$

$$\tau_w^{ref} = -\frac{m_{n11}m_{n22}}{n_w(m_{n21}+m_{n11})}\left(K_{pp}(\theta_p^{cmd} - \theta_p^{res}) + K_{dp}(\dot{\theta}_p^{cmd} - \dot{\theta}_p^{res}) + \ddot{\theta}_p^{cmd}\right) - \frac{m_{n11}}{n_w(m_{n21}+m_{n11})}\hat{\tau}_s^{dist}$$

$$K_{pp} = \frac{K_1}{K_2}, \quad K_{dp} = \frac{K_3}{K_2}$$

IV. Control

Fork Disturbance Observer (FDOB):

$$m_{41}\ddot{\theta}_w + m_{42}\ddot{\theta}_p + m_{43}\ddot{d}_m + m_{44}\ddot{\theta}_a + h_4 + g_4 = n_a\tau_a - T_{la}$$

$$m_{n44}\ddot{\theta}_a^{res} = n_a\tau_a^{ref} - \widetilde{\tau}_a^{dist}$$

$$\widetilde{\tau}_a^{dist} = m_{41}\ddot{\theta}_w^{res} + m_{42}\ddot{\theta}_p^{res} + m_{43}\ddot{d}_m^{res} + (m_{44} - m_{n44})\ddot{\theta}_a^{res} + h_4 + g_4 + T_{la}$$

$$\hat{\tau}_a^{dist} = \frac{g_a}{s + g_a}(n_a\tau_a^{ref} + g_a m_{n44}\dot{\theta}_a^{res}) - g_a m_{n44}\dot{\theta}_a^{res}$$

→ Pseudo differentiation

PD controller fork angle:

$$\tau_a^{ref} = K_{pa}(\theta_a^{cmd} - \theta_a^{res}) + K_{da}(\dot{\theta}_a^{cmd} - \dot{\theta}_a^{res}) + \hat{\tau}_a^{dist}$$

IV. Control

Fork Reaction Torque Observer (FRTOB):

$$T_{la} = \widetilde{\tau}_a^{ext} + \widetilde{\tau}_a^{fric}$$

$$\widetilde{\tau}_a^{reac} = m_{41}\ddot{\theta}_w^{res} + m_{42}\ddot{\theta}_p^{res} + m_{43}\ddot{d}_m^{res} + (m_{44} - m_{n44})\ddot{\theta}_a^{res} + h_4 + \widetilde{\tau}_a^{ext}$$

$$m_{n44}\ddot{\theta}_a^{res} = n_a\tau_a^{ref} - g_4 - \widetilde{\tau}_a^{fric} - \widetilde{\tau}_a^{reac}$$

$$\hat{\tau}_a^{reac} = \frac{g_r}{s + g_r}(n_a\tau_a^{ref} + g_r m_{n44}\dot{\theta}_a^{res} - g_4 - \widetilde{\tau}_a^{fric}) - g_r m_{n44}\dot{\theta}_a^{res}$$

Pseudo differentiation

$$\mathrm{t_l} = -\hat{\tau}_a^{reac}$$

IV. Control

Lift Disturbance Observer (LDOB):

$$m_{31}\ddot{\theta}_w + m_{32}\ddot{\theta}_p + m_{33}\ddot{d}_m + m_{34}\ddot{\theta}_a + h_3 + g_3 = f_m - F_{lm}$$

$$m_{n33}\ddot{d}_m^{res} = f_m^{ref} - \widetilde{f}_m^{dist}$$

$$\widetilde{f}_m^{dist} = m_{31}\ddot{\theta}_w^{res} + m_{32}\ddot{\theta}_p^{res} + (m_{33} - m_{n33})\ddot{d}_m^{res} + m_{34}\ddot{\theta}_a^{res} + h_3 + g_3 + F_{lm}$$

$$\hat{f}_m^{dist} = \frac{g_m}{s + g_m}(f_m^{ref} + g_m m_{n33}\dot{d}_m^{res}) - g_m m_{n33}\dot{d}_m^{res}$$

→ Pseudo differentiation

PD controller lift displacement:

$$f_m^{ref} = K_{pm}(d_m^{cmd} - d_m^{res}) + K_{dm}(\dot{d}_m^{cmd} - \dot{d}_m^{res}) + \hat{f}_m^{dist}$$

IV. Control

Lift Reaction Force Observer (LRFOB):

$$F_{lm} = \widetilde{f}_m^{ext} + \widetilde{f}_m^{fric}$$

$$\widetilde{f}_m^{reac} = m_{31}\ddot{\theta}_w^{res} + m_{32}\ddot{\theta}_p^{res} + (m_{33} - m_{n33})\ddot{d}_m^{res} + m_{34}\ddot{\theta}_a^{res} + h_3 + \widetilde{f}_m^{ext}$$

$$m_{n44}\ddot{d}_m^{res} = f_m^{ref} - g_3 - \widetilde{f}_m^{fric} - \widetilde{f}_m^{reac}$$

$$\hat{f}_m^{reac} = \frac{g_r}{s + g_r}\left(f_m^{ref} + g_r m_{n33}\dot{d}_m^{res} - g_3 - \widetilde{f}_m^{fric}\right) - g_r m_{n33}\dot{d}_m^{res}$$

Pseudo differentiation

$$\mathrm{m_l} = \frac{\hat{f}_m^{reac}}{g\cos(\theta_p)}$$

IV. Control

Wheel Position Control:

$$\theta_p^{cmd-PD} = K_{pw}(\theta_w^{cmd} - \theta_w^{res}) + K_{dw}(\dot{\theta}_w^{cmd} - \dot{\theta}_w^{res})$$

Total pitch command:

$$\begin{cases} \theta_p^{cmd} = \theta_p^{cmd-IK} + \theta_p^{cmd-PD} & \text{Z trajectory generation} \\ \theta_p^{cmd} = \theta_p^{cmd-ID} + \theta_p^{cmd-PD} & \text{X trajectory generation} \end{cases}$$

V. Results

Parameter	Explanation	Value
K_{pp}	P-gain of pitch angle control	200
K_{pd}	D-gain of pitch angle control	28.3
K_{pa}	P-gain of arm position control	200
K_{da}	D-gain of arm position control	50
K_{pm}	P-gain of lift position control	200
K_{dm}	D-gain of lift position control	50
K_{pw}	P-gain of wheel position control	0.07
K_{dw}	D-gain of wheel position control	0.09
g_s (rad/s)	Cutoff angular frequency of SPADO	$2\pi 4$
g_a (rad/s)	Cutoff angular frequency of arm FDOB	$2\pi 5$
g_r (rad/s)	Cutoff angular frequency of FRTOB, LRFOB	$2\pi 1$
g_m (rad/s)	Cutoff angular frequency of LDOB	$2\pi 4$
N_w	Wheel gear ratio	11
N_a	Arm gear ratio	33

Parameter	Explanation	Value
I_{wy} (kg m^2)	Wheel inertia	0.0052
I_{by} (kg m^2)	Body inertia	0.5407
I_{my} (kg m^2)	Lift inertia	0.0482
I_{ay} (kg m^2)	Arm inertia	0.0890
l_b (m)	Body CoG distance	0.1663
l_m (m)	Lift CoG distance	0.3975
l_a (m)	Arm CoG distance	0.2200
m_w(kg)	Wheel mass	1.21
m_b (kg)	Body mass	43.1
m_m (kg)	Lift mass	21.5
m_a (kg)	Arm mass	3.5
m_l (kg)	Load mass	5

V. Simulation

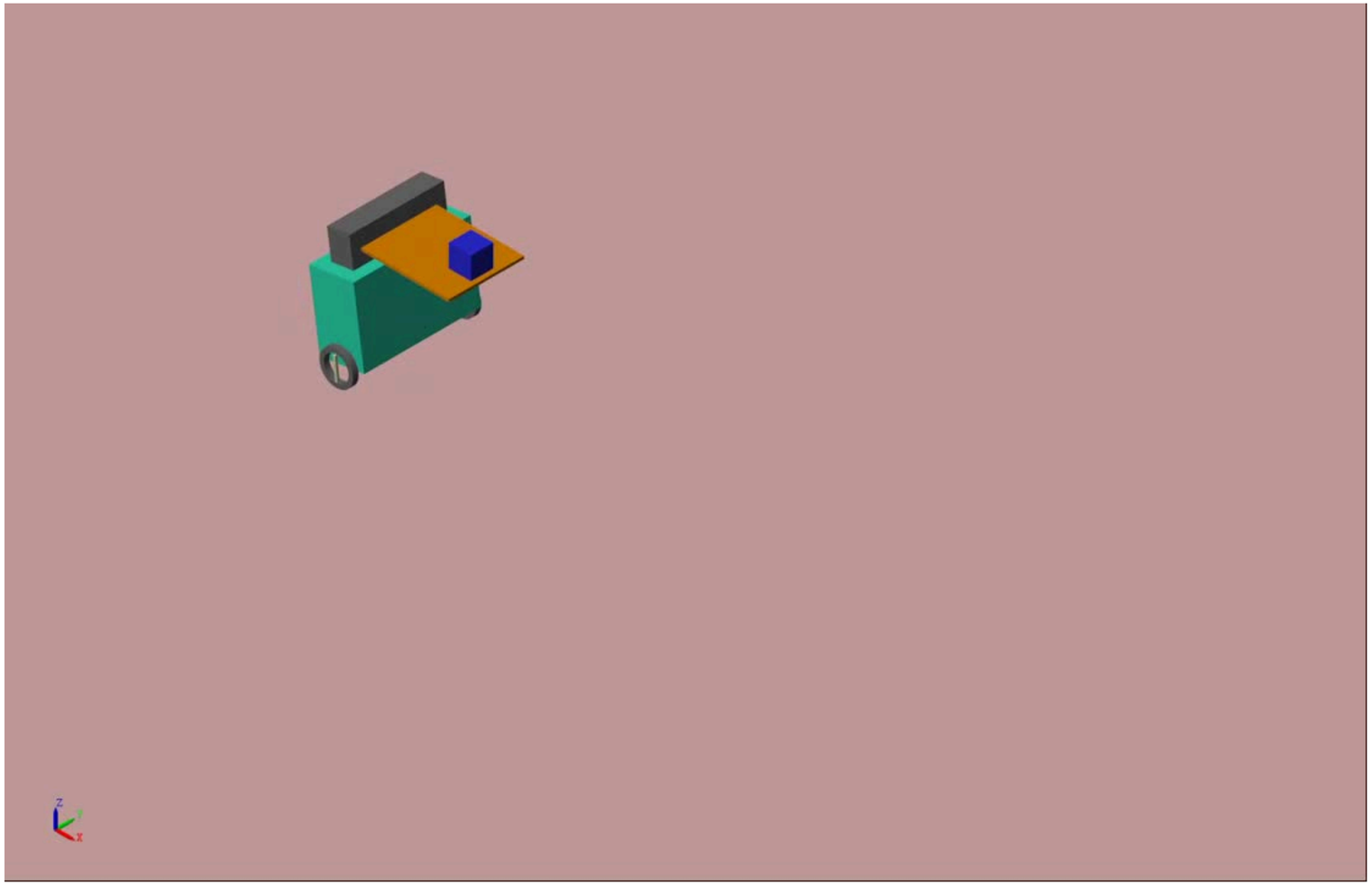

V. Simulation

Horizontal displacement of the robot

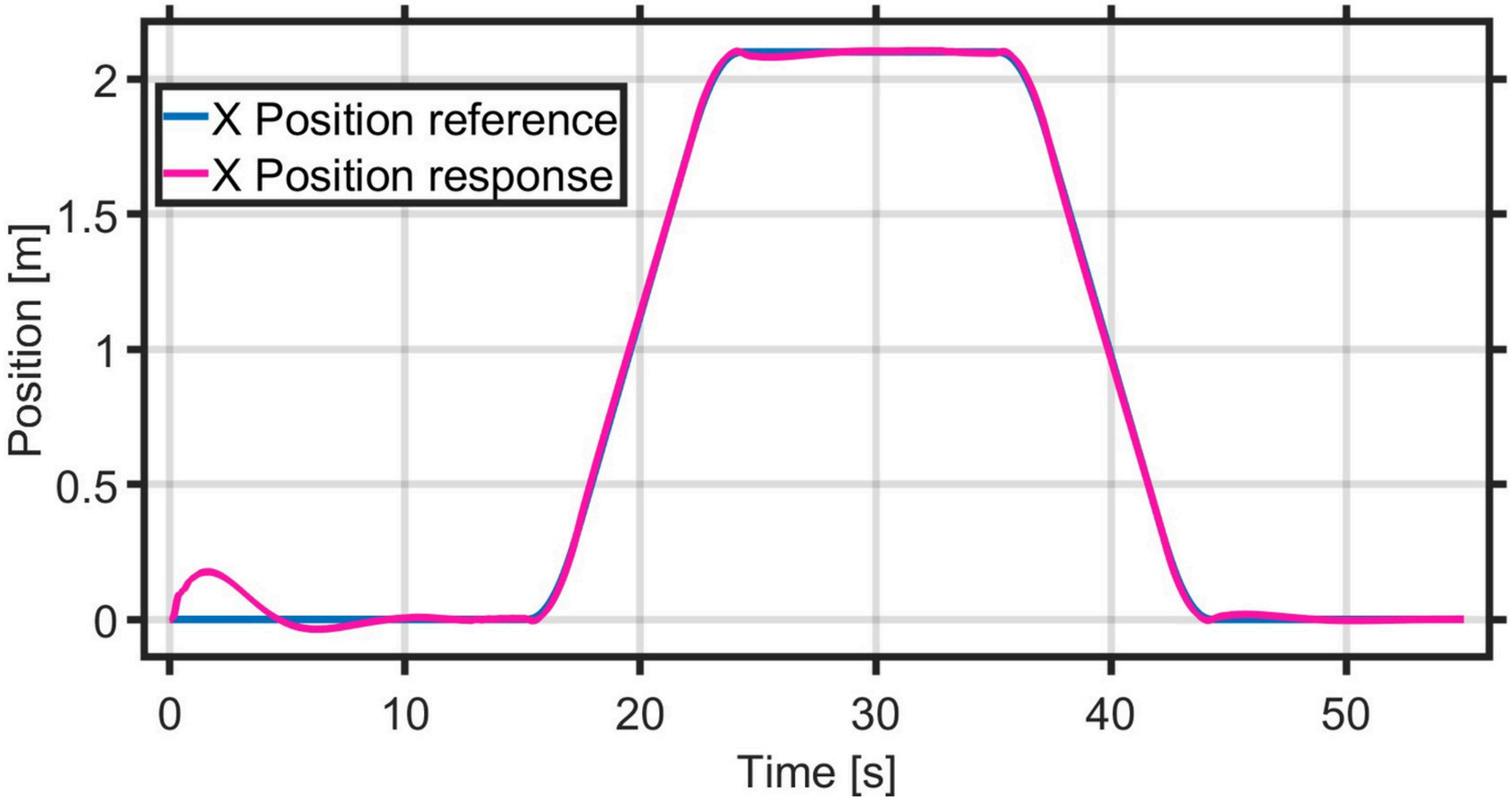

V. Simulation

Position error of the robot

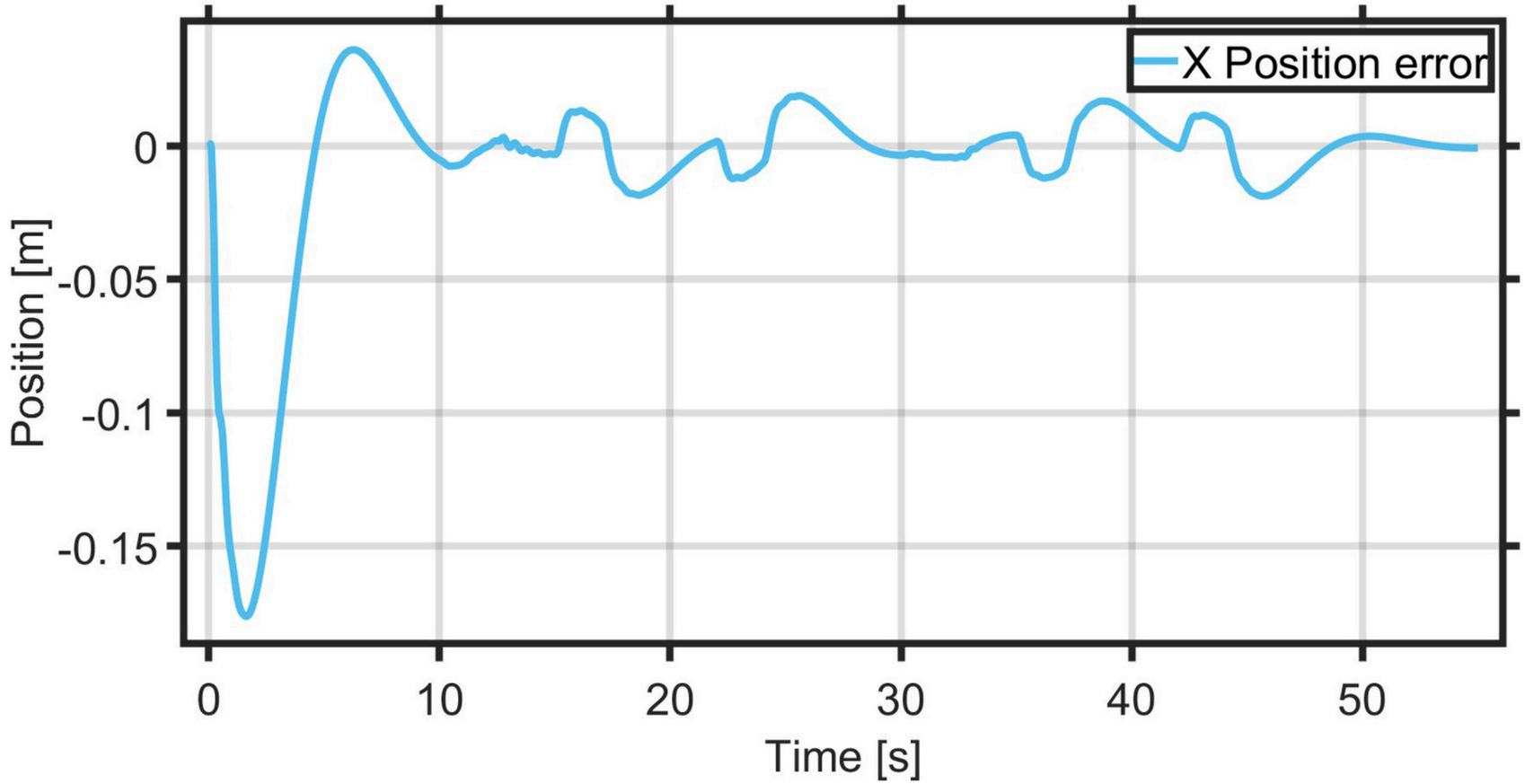

V. Simulation

Horizontal velocity of the robot

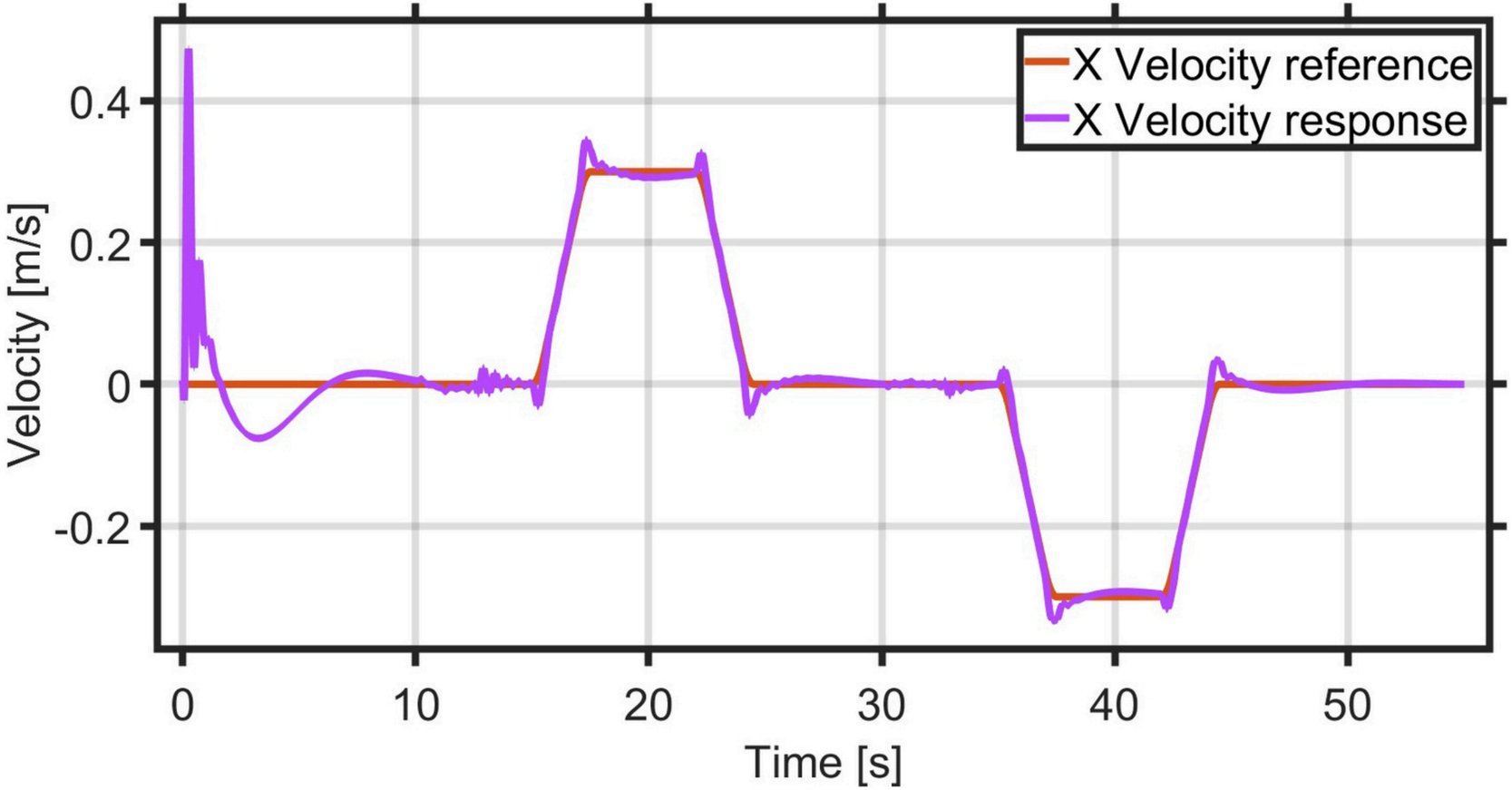

V. Simulation

Vertical position of the fork

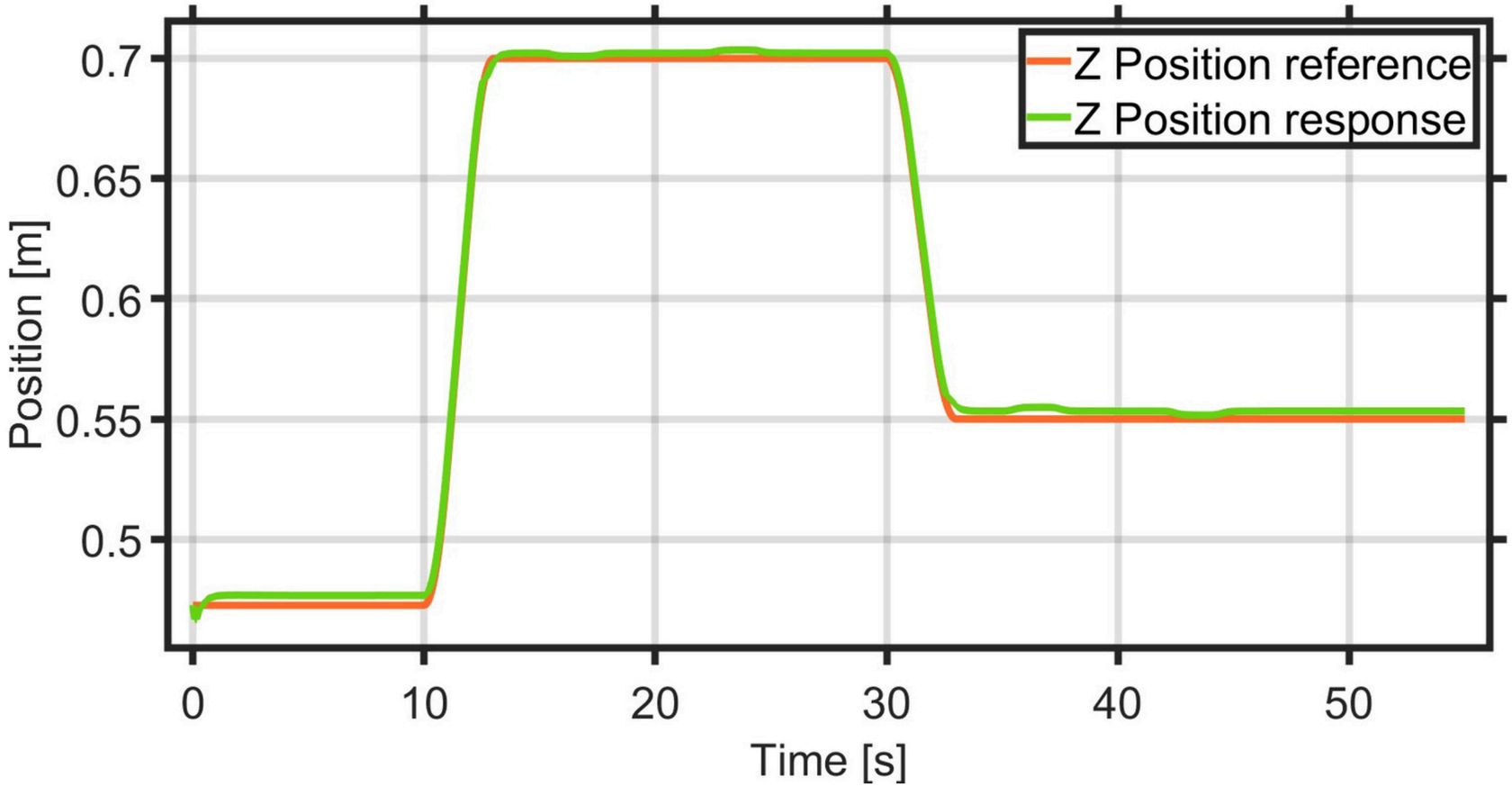

V. Simulation

Estimated external torque over the fork

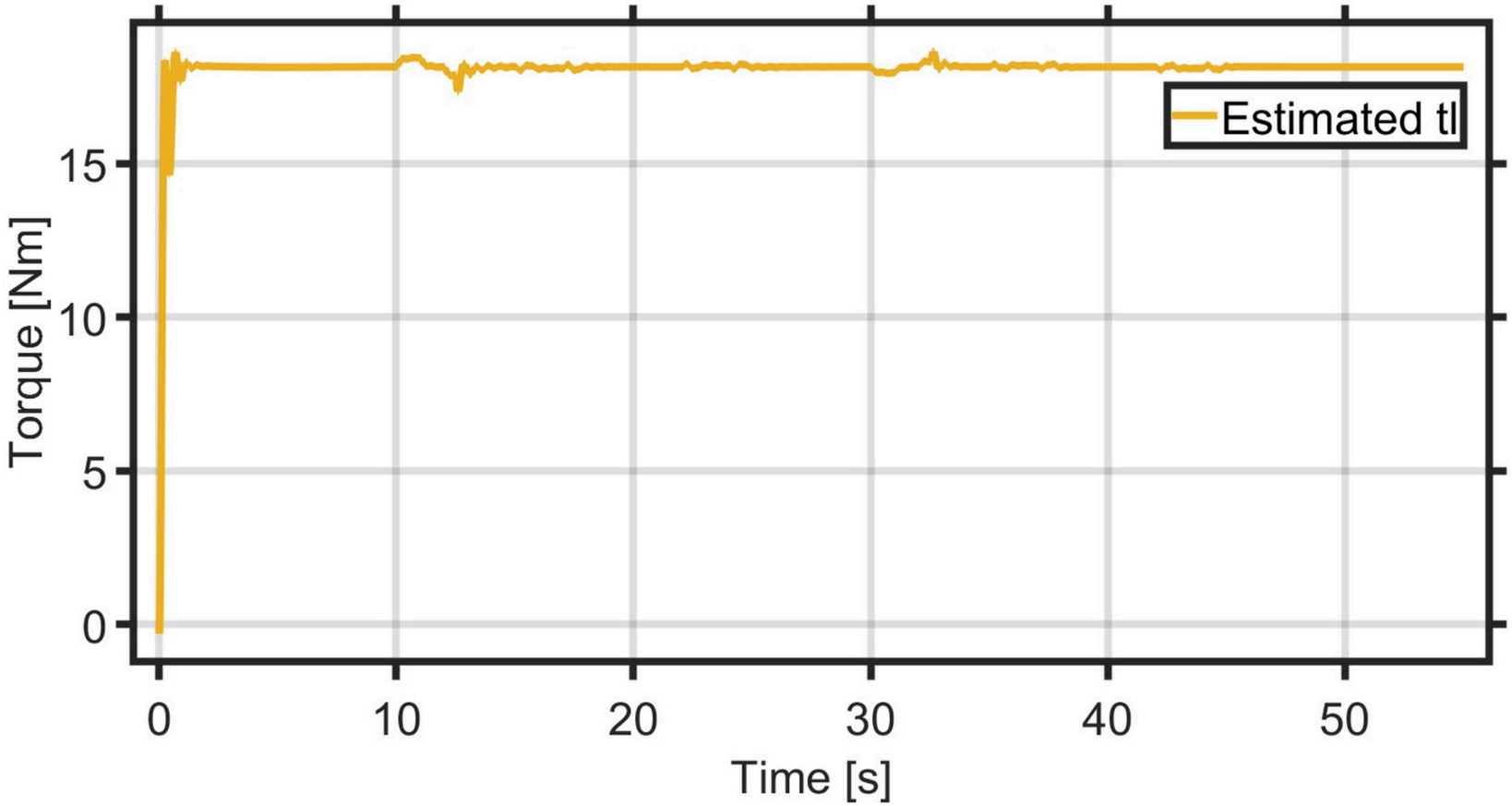

V. Simulation

Estimated mass of the external load

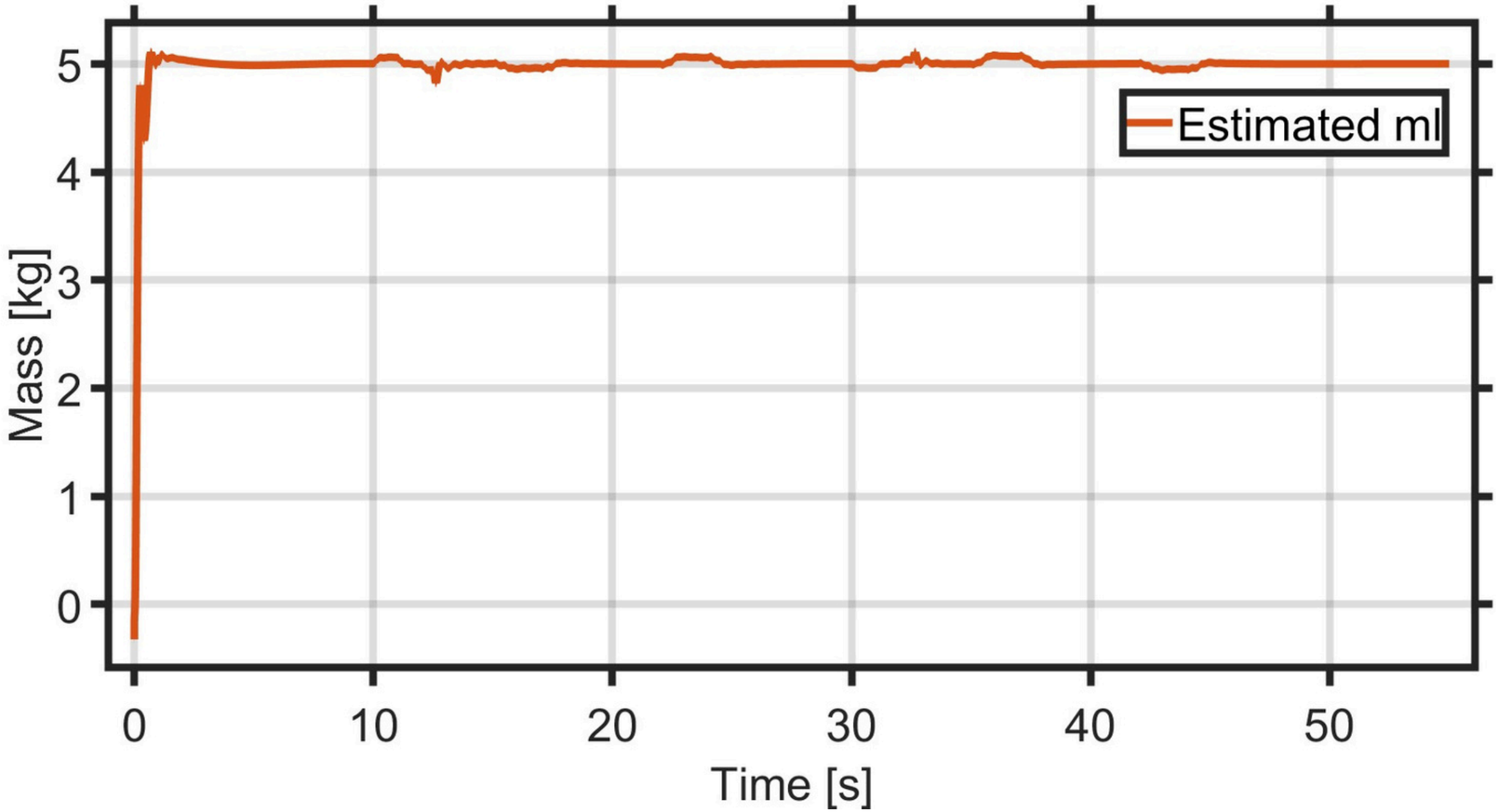

VI. Conclusions and Future work

- The proposed motion planning and control strategies are capable of generating trajectories that the TWFR is capable of executing with an admissible position error.
- The implementation of adaptive IK and ID solutions that depend on the estimation of physical properties of the external load provides great flexibility in industrial environments where it is not possible to control the variables of the load that will be manipulated.
- The next steps for this work are the detailed mechanical design and construction of the lift subsystem. With the complete TWFR, the mathematical modeling and control parameters must be adapted to match the real system to test physically the presented motion planning and control algorithms.

References

[1] H. Kanazawa, K. Ishizaki, Y. Miyata, M. Nawa, N. Kato, and T. Murakami, "Model-Based Pitch Angle Compensation for Center of Gravity Variation in Underactuated System with an Arm," in Proceedings of the 2023 IEEE 32nd International Symposium on Industrial Electronics (ISIE), 2023, pp. 1-6.
[2] H. Yajima, K. Ishizaki, Y. Miyata, M. Nawa, N. Kato, and T. Murakami, "Posture Stabilization Control Compensating Variation of Body Center of Gravity in Underactuated System," in Proceedings of the 2023 IEEE International Conference on Mechatronics (ICM), 2023, pp. 1-6.
[3] J. Ito and T. Murakami, "Underactuated Control for Two-Wheeled Mobile Robot with an Arm Using Torque Constraint Conditions and Disturbance Observer," in Proceedings of the 2023 IEEE 32nd International Symposium on Industrial Electronics (ISIE), 2023, pp. 1-6.
[4] Mezawa, M. (2022). Virtual Suspension Control in Two-Wheeled Transport Robot (Master's thesis, Keio University).
[A] https://www.flaticon.com/free-icons/comparison
[B] https://www.flaticon.com/free-icons/standard
[C] https://www.flaticon.com/free-icons/storage

Thank you!